algorithms

MDPI

Article

Region-Based Algorithm for Switching Frequency Reduction in Predictive Control of Converter Supplied Electric Drives

Manuel R. Arahal [1,†], Manuel G. Satué [1,*,†], Francisco Colodro [2] and Alfredo P. Vega-Leal [2]

[1] Systems Engineering and Automation Department, University of Seville, 41092 Seville, Spain; arahal@us.es
[2] Electronic Engineering Department, University of Seville, 41092 Seville, Spain; pcolr@us.es (F.C.); alperez@us.es (A.P.V.-L.)
* Correspondence: mgarrido16@us.es; Tel.: +34-954-487-343
† These authors contributed equally to this work.

Abstract

Switching losses make up for a notable portion of all losses in converter-supplied electric drives. Control algorithms such as Finite State Model Predictive Control (FSMPC) have tackled this issue in different ways; in particular incorporating a switching penalty to the cost function. This, however, results in an optimization problem with increased computational load, restricting the attainable sampling frequency for a given computing hardware. Recently, fast algorithms have been developed that reduce the computational load. However they cannot incorporate the switching penalty term. This paper explores a way around this problem for the particular case of stator current control of a five-phase induction motor. The proposal achieves fast computation even if a term for switching frequency reduction is present in the cost function. Experimental results show how stator current tracking performance is affected in both the torque producing plane and the harmonic subspace.

Keywords: Finite State Model Predictive Control; variable speed drives; induction motor; multi-phase drives

1. Introduction

Recent advances in the control of electrical systems using power converters rely on the use of Model Predictice Control (MPC) [1–3]. In particular, Finite State Model Predictive Control (FSMPC) is very relevant in the specialized literature. FSMPC is based on the optmization of a Cost Function (CF) made each sampling period. The CF is constructed by adding terms that penalize deviations of variables from their objectives. The adjective predictive is used because the variables used in the CF are predictions obtained from a model of the plant.

A case of special interest is that of multiphase systems. For a number of phases greater than 3, the power distribution, reliability and current quality are enhanced [4]. The FSMPC technique has been applied to those systems. The cost function uses (typically) the following terms. First, the tracking error in the torque producing plane (i.e., $\alpha - \beta$ plane). Second, the regulation error in the harmonic plane (i.e., $x - y$ plane). Third, the instantaneous switch changes at the power converter. These three elements represent three different objectives for the sample-wise optimization. Weighting factors (WFs) are used to combine those terms into a single CF. The WFs allow for accommodating variables with different units. They can also be used to put more emphasis on some objectives over the rest. For instance, the Average Switching Frequency (ASF) should be maintained below the limits of the converter, which depends on the technology it uses (e.g., standard IGBT, SiC, GaN).

Check for updates

Academic Editor: Sheng Du

Received: 1 April 2026
Revised: 4 May 2026
Accepted: 7 May 2026
Published: 9 May 2026

Copyright: © 2026 by the authors. Licensee MDPI, Basel, Switzerland. This article is an open access article distributed under the terms and conditions of the Creative Commons Attribution (CC BY) license.

In order to put the proposal in the appropriate context it is useful to consider how FSMPC has developed recently. First note that the optimization of the cost function in FSMPC is usually done by exhaustive search over the space of converter configurations [5,6]. Said space contains just a handful of elements determined by the on/off position of the discrete switches. The resulting voltage for each configuration is termed Basic Voltage Vector (BVV), depicted in Figure 1. The changes in the switch positions from one sampling period to the next determine the ASF. The way ASF has been tackled follows two distinct paths. In one of them, researchers rely on carefully tuning the corresponding WF (i.e., the WF multiplying the switching term). The problem with this approach is that fast optimization algorithms do not work with CFs that include the switching term. As a result, the computational load is high, which entails a reduction in sampling frequency [7]. In addition, the WF selection procedures have stagnated in the past up until the recent introduction of flexible, low complexity online WF selection procedures [8–10].

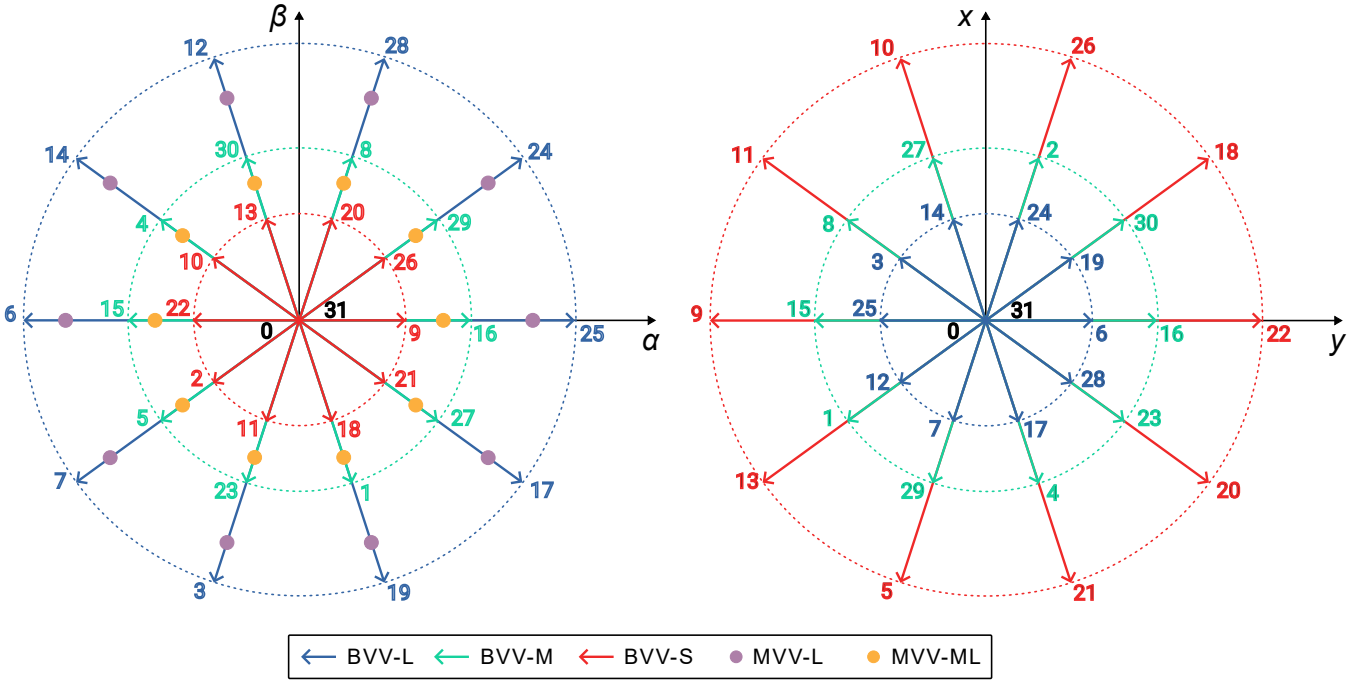


Figure 1. Basic Voltage Vectors and Multi Voltage Vectors in $\alpha - \beta$ and $x - y$ subspaces.

It must be noted that this path has its opposite side proposing WF elimination [11]. This has been used as a means of simplifying CF design. For instance, in [12] analytical normalization is proposed. Quadratic prediction and the design of constraints are used in [13], achieving a reduction in the ASF at the cost of increased computational load. There are also intermediate solutions where the full exploration of switching states is avoided, as in [14].

A special case of FSMPC uses more than one BVV per sampling period. This family of techniques is referred to as the multivector approach (MVV in Figure 1). The WF can be eliminated, producing a reduction in computational load. In addition, the ASF has been treated by a pre-selection of input sequences [15]. In [16], a dead-beat method with hybrid exploration state is used to reduce computational burden and reduce current ripple. Similar works use asymmetric space vector pulse width modulation [17] and reduced candidate vectors [18]. In [19], the dead-beat concept is used in the controller for both speed and current control. Similar schemes have been proposed in [20]. Computational load and ASF reduction are also tackled in works dealing with the virtual voltage vector

technique [21–23]. The dead-beat concept has also been used to tackle the problem of harmonics in series-winding topology [24].

Single vector FSMPC approaches did not use fast methods for CF optimization until recently. The problem is especially acute in multi-phase drives since the number of VV grows exponentially with the number of phases [25]. The set of attempts to diminish the computational load include: reduction of the active VV set [26], simplification of the combinatorial search [27], use of specialized hardware [28], and use of model-free approaches [29]. Region-based methods have been recently proposed to obtain the control move in one go. For instance, in [30], current control of a three-level inverter is done by dividing the space vector set into sectors. The authors proposed a similar idea for multi-phase systems [31]. This constitutes an extension of previous works that use geometrical insights to reduce the computational load [32]. Other works have proposed neural networks [33] to solve the optimization with reduced load.

However, in these previous works, the harmonic subspace was not considered in full with a proper WF. This has been corrected in [34], where a hyperplane partition is used to optimize the CF in one go. Despite these efforts, a low computational load algorithm for the full cost function (i.e., including all three terms) has not been developed.

Contributions

The state of the art shows a need for fast FSMPC algorithms that can deal with the switching frequency term of the cost function. Of course, the solution must not forget about harmonic $(x - y)$ content treatment in closed loop. This goal has been elusive for a number of years where partial solutions have been reported.

The proposed method is a region-based algorithm for cost function optimization. As such it can eliminate the exhaustive search that is still in use in other approaches. As a result the sampling times can be reduced. This fact grants significant advantages as is noted in discrete-time control theory.

The proposed method retains weighting factors as a means to adapt the solution to the specific needs of each application. This means that the trade-off between figures of merit can be balanced via WF selection. In this way the proposal benefits from recent advances in WF tuning. Also, the proposal adds very little computational load to the basic FSMPC method. In this way the attainable sampling frequencies are not reduced.

We note that previous approaches have two drawbacks: (1) they need the application of various Basic Voltage Vectors per sampling period, increasing the number of commutations per sampling period, thus limiting the sampling time, and (2) they lack flexibility to trade switching frequency with other performance indicators. The proposed method eliminates those problems. Furthermore, the full set of basic VV can be used with no reduction in the number of candidate vectors.

In the next section, the FSMPC control structure is explained. Later, some background on the fast optimization method is presented (Section 3), followed by the proposal of a fast FSMPC capable of switching frequency. The experimental results, discussion and conclusions end the paper.

2. Background

The proposal is for multiphase systems. In this paper a five-phase induction motor is considered. In the following, a short review of the basic elements of FSMPC is presented to put the contribution into context.

2.1. FSMPC Elements

The elements of the FSMPC technique are the model and the cost function. A diagram of the FSMPC technique is shown in Figure 2. For the sake of clarity the variables used in the diagram are introduced now. The mechanical speed is ω_m and is measured in the motor and compared with the reference ω_m^*. The speed loop determines the quadrature current reference i_{qs}^* which is converted to a torque producing plane ($\alpha - \beta$) and a non-torque producing plane ($x - y$) by means of the Park transformation matrix T_p^{-1}. The direct component i_{ds}^* is independently set using the Indirect Field Oriented Control method [35].

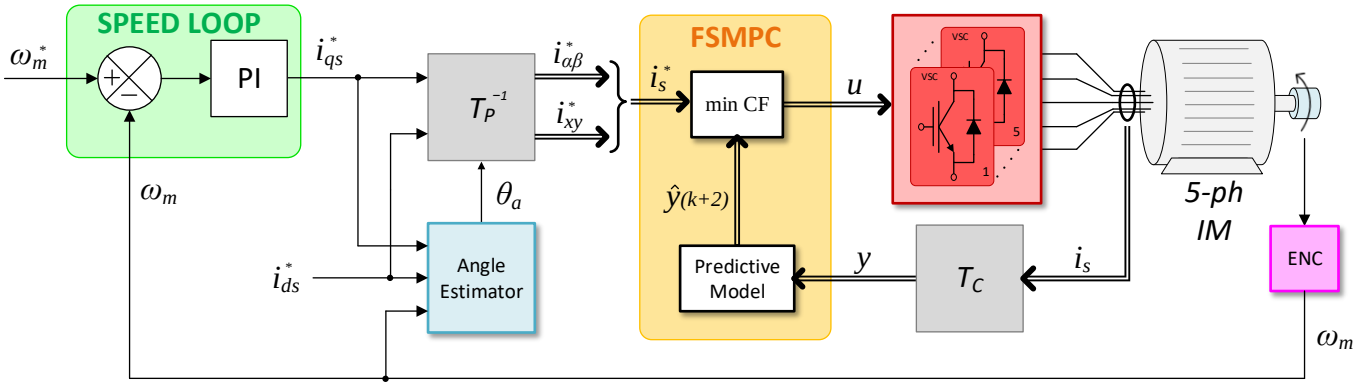


Figure 2. FSMPC diagram.

The control variable u is obtained by minimizing the Cost Function (CF). In FSMPC it consists of a vector with the state K of the VSI switches for each phase. Since the motor considered here has 5 phases, a-b-c-d-e, the control signal is $u = (K_a, K_b, \cdots, K_e)^\top$, where each K_i represents the state (or/off) of one of the switches for leg i at the VSI. The other switch has the complementary state so it does not need to be specified. Only two values are possible for each K_i, either 0 or 1. Then the number of distinct values for u ranges from $(0,0,0,0,0)$ to $(1,1,1,1,1)$. These produce the 32 basic voltage vectors shown in Figure 1 and are denoted by the decimal number corresponding to the binary components of u.

The controlled variable is y, consisting of the measured stator current i_s transformed to $\alpha - \beta - x - y$ coordinates by means of the Clarke T_c matrix.

$$T_c = \frac{2}{5}\begin{pmatrix} 1 & \cos 1\vartheta & \cos 2\vartheta & \cos 3\vartheta & \cos 4\vartheta \\ 0 & \sin 1\vartheta & \sin 2\vartheta & \sin 3\vartheta & \sin 4\vartheta \\ 1 & \cos 2\vartheta & \cos 4\vartheta & \cos 1\vartheta & \cos 3\vartheta \\ 0 & \sin 2\vartheta & \sin 4\vartheta & \sin 1\vartheta & \sin 3\vartheta \end{pmatrix}, \tag{1}$$

where $\vartheta = 2\pi/5$. A prediction of y is provided by the predictive model as $\hat{y}$. The discrete-time predictive model of the motor is obtained from first principles and can be expressed as

$$\hat{y}(k+1) = C(\omega)y(k) + BV(k) \tag{2}$$

where matrices C and B are found by time discretization with sampling time T_s. This gives $C = (I + A_c T_s)$, and $B = T_s B_c$, where

$$A_c = \begin{pmatrix} a_2 & -a_4 & 0 & 0 \\ a_4 & a_2 & 0 & 0 \\ 0 & 0 & a_3 & 0 \\ 0 & 0 & 0 & a_3 \end{pmatrix}, \quad B_c = \begin{pmatrix} c_2 & 0 & 0 & 0 \\ 0 & c_2 & 0 & 0 \\ 0 & 0 & c_3 & 0 \\ 0 & 0 & 0 & c_3 \end{pmatrix}. \tag{3}$$

The coefficients used are: $c_1 = L_s L_r - L_M^2$, $c_2 = L_r/c_1$, $c_3 = 1/L_{ls}$, $c_4 = L_M/c_1$, $a_2 = -R_s c_2$, $a_3 = -R_s c_3$, $a_4 = -L_M c_4 \omega_r$, $a = 4/5$, $b = -1/5$, $c = -b$, $d = 2/5$, $a_{r4} = R_r c_4$, $a_{l4} = L_r c_4 \omega_r$. The values for the experimental setup are shown in Table 1.

Table 1. Parameters of the induction motor.

Parameter	Symbol	Value	Units
Stator resistance	R_s	12.85	Ω
Rotor resistance	R_r	4.80	Ω
Stator leakage inductance	L_{ls}	79.93	mH
Rotor leakage inductance	L_{lr}	79.93	mH
Mutual inductance	L_M	681.7	mH
Number of pairs of poles	P	3	-

From Equation (2) the two-step-ahead prediction of the stator currents can be found as

$$\hat{y}(k+2) = A(\omega)\hat{i}(k+1) + BV(k+1) \tag{4}$$

where V is the voltage produced by the control action u, defined as $V = \left(v_{s\alpha}, v_{s\beta}, v_{sx}, v_{sy}\right)$ and that can be computed by means of

$$V(k+1) = V_{DC} u(k+1) T T_c^{-1} \tag{5}$$

where V_{DC} is the DC-link voltage and T is the connectivity matrix of the 5-phase VSI.

The control signal is found minimizing a cost function such as

$$J(k+2) = \|\hat{e}_{\alpha-\beta}(k+2)\|^2 + \lambda_{xy}\|\hat{e}_{x-y}(k+2)\|^2 + \lambda_{sc} SC(k+1) \tag{6}$$

In (6) Parameter λ_{xy} is a WF. It allows trading $\alpha - \beta$ tracking accuracy for $x - y$ content. Similarly, λ_{sc} is the weighting penalizing changes in the converter switches (either on/off or off/on). The term SC stands for switch changes and is computed considering the components of $u(k)$ and $u(k+1)$ as indicated

$$SC(k+1) = \sum_j |K_j(k+1) - K_j(k)|. \tag{7}$$

2.2. Fast Optimization Algorithm

The basic FSMPC method uses exhaustive exploration to minimize the cost function (6). In this paper the VSI has five phases to supply the 5-phase induction motor. This can be seen as an especially demanding case compared with the usual 3-phase case. In a five-phase system, the number of BVVs is 32. The exhaustive exploration must compute J for each possible BVV and select the one producing the minimum value of J. This is computationally intensive. However, multiphase systems posses attractive traits as explained in the introduction. So one has to find a way to accelerate the optimization phase.

The method of [31] can produce the optimal control move without the 32 evaluations of the cost function. However, it just works for $\lambda_{sc} = 0$. The proposal of this paper uses the method of [31] to derive a candidate solution that is then checked in terms of switch changes. The solution is modified just in cases where the savings in terms of switch changes justify the predicted loss in current tracking. Before explaining the proposal it is convenient to recall the basics of the Fast FSMPC method (FFSMPC) proposed in [31].

The method uses the actual stator current measurement and the actual future reference to produce a set of indices that are later used in a Look Up Table (LUT) to produce the optimal voltage vector in one go, without iterations.

The first step is to define the gap ($g(k+1)$) as the error in current tracking if no voltage is applied during the $k+1$ period. This is found as

$$g(k+1) \doteq i^*(k+2) - A\hat{i}(k+1) \tag{8}$$

It is shown in [31] that $g(k+1)$ allows the computation of the optimal control signal $u(k+1)$ without iterations by using a Look Up Table (LUT). The components $g_{\alpha-\beta}$ and g_{x-y} are treated by considering weighted values for the control errors by using the parameters $W_{\alpha-\beta}$ and W_{xy}. At each sampling time, the subspace ($\alpha-\beta$ or $x-y$) that produces the largest deviations is used to define the actual LUT from which the control action is selected (either $\alpha-\beta$ or $x-y$). The selection of the control action is specified by the following algorithm:

1. Compute the one-step-ahead prediction as indicated by Equation (2).
2. Compute the gap according to its definition given by Equation (8).
3. Determine the control action according to the following steps:
   - 3.1. Compute $r_{\alpha-\beta} = \mid (g_\alpha, g_\beta) \mid$ and $r_{x-y} = \mid (g_x, g_y) \mid$.
   - 3.2. If $W_{xy} r_{x-y} < r_{\alpha-\beta}$ make $C_\sigma = 1$ so that the $\alpha-\beta$ LUT is used, else make $C_\sigma = 0$ to use the $x-y$ LUT.
   - 3.3. If $\sigma = 1$ compute Q the quadrant of (g_α, g_β) else Q is the quadrant of (g_x, g_y).
   - 3.4. Compute $\tau = \mid g_2/g_1 \mid$. If $\sigma = 1$ then $\tau = \mid g_\beta/g_\alpha \mid$, else $\tau = \mid g_y/g_x \mid$. Determine the case (C_τ) as $C_\tau = 1$ if $\tau \geq U_1$, $C_\tau = 2$ if $U_2 \leq \tau < U_1$ or $C_\tau = 3$ if $\tau < U_2$.
   - 3.5. If $C_\sigma = 1$ then $\rho = \sqrt{g_\alpha^2 + g_\beta^2}$, else $\rho = \sqrt{g_x^2 + g_y^2}$. Determine the case $C_\rho = 1$ if $\rho \geq G_L$, $C_\rho = 2$ if $G_M < \rho \leq G_L$, $C_\rho = 3$ if $G_S < \rho \leq G_M$, and or $C_\rho = 4$ $\rho < G_S$.
   - 3.6. Obtain the BVV index from Table 2 using the values of C_σ, C_τ, C_ρ and Q.

The control signal $u(k+1)$ is the one corresponding to the BVV selected in the process.

The method can be summarized as follows: from the actual stator current measurement and the future reference, compute indices C_σ, C_τ, C_ρ and Q. Now, the voltage vector to be applied (the optimal one) is denoted by a number from 1 to 32. Lets refer to this number as V_{opt}. Table is a means to produce the function $V_{opt} = f(C_\sigma, C_\tau, C_\rho, Q)$. Finally, function f is exactly determined by the LUT because the indices C_σ, C_τ, C_ρ and Q can take just a handful of discrete values that can be tabulated.

Table 2. Look Up Tables showing optimal Basic Voltage Vectors.

$C_\sigma = 1$						$C_\sigma = 0$					
C_τ	C_ρ	$Q=1$	$Q=2$	$Q=3$	$Q=4$	C_τ	C_ρ	$Q=1$	$Q=2$	$Q=3$	$Q=4$
1	1	29	13	4	20	1	1	27	11	6	22
1	2	9	31	24	2	1	2	3	28	30	5
1	3	21	14	12	19	1	3	25	25	8	18
1	4	1	1	1	1	1	4	1	1	1	1
2	1	25	15	8	18	2	1	19	12	14	21
2	2	30	5	3	28	2	2	31	9	2	24
2	3	27	11	6	22	2	3	20	4	13	29
2	4	1	1	1	1	2	4	1	1	1	1
3	1	26	7	7	26	3	1	23	10	10	23
3	2	17	16	16	17	3	2	17	16	16	17
3	3	10	23	23	10	3	3	7	26	26	7
3	4	1	1	1	1	3	4	1	1	1	1

3. Proposal

The FFSMPC method of Section 2.2 allows the fast computation of the control signal for the particular case $\lambda sc = 0$. The proposal uses this first approximation as a stepping stone to compute a solution that balances $\alpha - \beta - x - y$ tracking with switch changes.

In order to describe the algorithm let us denote as u^{o1} the control action found by the FFSMPC method. The number of associated switch changes (SC^{o1}) is found using Equation (7) with $u(k+1) = u^{o1}$. Now, if this value is zero, it means that the solution of the FFSMPC is also the solution for the complete cost function. This is because the SC term cannot take negative values.

If $SC^{o1} > 0$, then one can consider trading switch changes with tracking error. This trading can be achieved by limiting commutations. The price to pay for having less commutations is an increase in tracking error. To quantify this, one can consider the extreme case of restricting $SC(k+1)$ to be zero. Then $u(k+1)$ must be equal to $u(k)$. For the sake of clarity this control action is denoted as u^{o0}. Notice that u^{o1} is optimal in the sense of $\alpha - \beta - x - y$ tracking, whereas u^{o0} is optimal in terms of the number of switch changes. Both control actions u^{o0} and u^{o1} can be thought to be candidates. By choosing one it is possible to compute the associated cost using (6). The trade-off can be solved by issuing the solution that provides the lesser value for J. The idea is simple but it can be carried one step further as explained below.

In addition to u^{o0}, one can also consider the case when just one switch change is allowed, so that $SC(k+1) = 1$. Of course, this only makes sense in cases where $SC^{o1} > 1$. Now, forcing just one switch change means that $u(k+1)$ and $u(k)$ differ in just one position. For any given value of $u(k)$ there are 5 different values of $u(k+1)$ satisfying this requisite. Again, the associated cost can be computed and the trade-off is solved.

It is interesting to notice that candidate solutions containing changes that are not present in u^{o1} can be disregarded. This means that the number of possible BVVs differing from the previous one in just one position that need be considered is not 5 but just SC^{o1}. Now, SC^{o1} is always $SC^{o1} \leq 5$. Also, it is very rare to encounter a case with $SC^{o1} > 3$. This is important because the proposed method revolves around considering these candidate solutions and their associated J values. This means that it is important that they represent a number much less than the 32 control moves of basic FSMPC.

With these considerations the algorithm for the proposed method can be described as follows.

1. Determine u^{o1} using the FFSMPC method of Section 2.2.
2. Compute SC^{o1} using Equation (7) with $u(k+1) = u^{o1}$.
3. If $SC^{o1} = 0$ set $u(k+1) = u^{o1}$ and end, else continue.
4. Determine the set $\mathbb{S}$, which contains all possible control actions needing a number of switch changes $SC \leq 1$.
5. Trim those elements in $\mathbb{S}$ needing switch changes that are not present in u^{o1}.
6. For each remaining element in $\mathbb{S}$ compute the cost using (6).
7. Select $u(k+1)$ as the element in $\mathbb{S}$ that provides the minimum cost.

4. Experimental Results and Discussion

The experiments are carried out using a laboratory setup that is described in the following. The main element is a five-phase induction motor with parameters shown in Table 1. The rest of elements include the five-phase inverter fed by a DC power supply operating at 300 V. The five-phase VSI is constructed by using two conventional three-phase VSIs. The total number of available phases is six, from which just five are used to power the a-b-c-d-e phases of the induction motor.

The control program runs in a Digital Signal Processor (DSP) TMS320F28335 (Texas Instruments (TI), Dallas, United States). The input signals come from Hall sensors that are used to measure the stator phase currents. The references are supplied to the DSP using a computer. The computer is also used for the logging of variables. A diagram of the setup is shown in Figure 3.

The performance indicators used for assessment are the usual in multiphase systems. These include the Root Mean Squared (RMS) control error in $\alpha - \beta$ and $x - y$ planes and the Average Switching Frequency (ASF). These are described below.

$$E_{\alpha-\beta} = \sqrt{\frac{1}{(k_2 - k_1 + 1)} \sum_{k=k_1}^{k_2} e_{\alpha-\beta}^2(k)} \tag{9}$$

$$E_{x-y} = \sqrt{\frac{1}{(k_2 - k_1 + 1)} \sum_{k=k_1}^{k_2} e_{xy}^2(k)} \tag{10}$$

$$ASF = \frac{1/(2 \cdot 5)}{T_s(k_2 - k_1 + 1)} \sum_{k=k_1}^{k_2} SC(k) \tag{11}$$

where $e_{\alpha-\beta}$ represents the tracking error for the $\alpha - \beta$ plane. Similarly, e_{xy} represents the tracking error in the $x - y$ subspace.

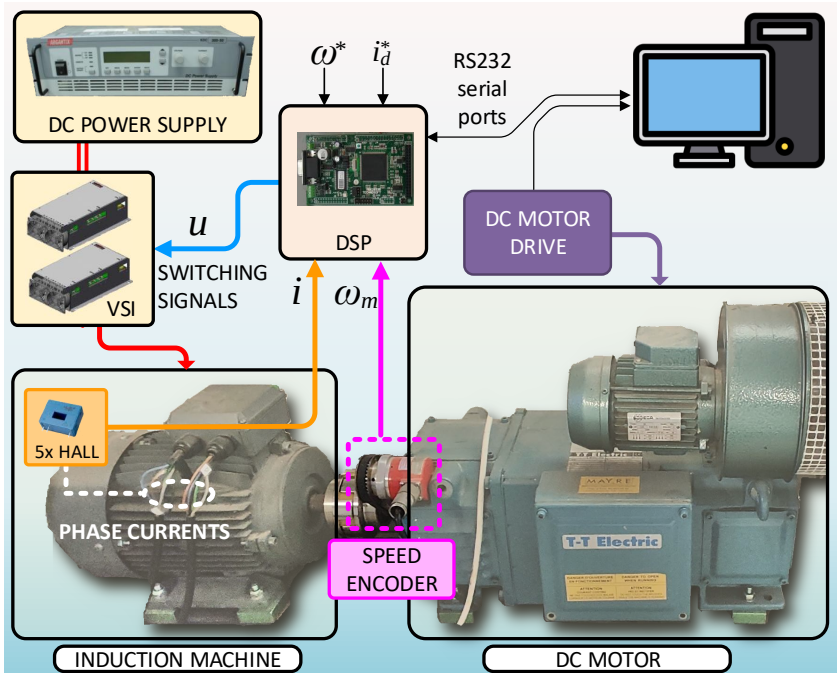


Figure 3. Diagram of the laboratory setup.

The quantities in (9)–(11) are average values found for discrete-time indices k_1, k_2. In the experiments k_1, k_2 cover four electric cycles. In this way the averages are statistically sound.

The proposed control algorithm is compared against: (1) a standard FSMPC method using the full cost function of (6) and (2) a multi-vector FSMPC method based on Virtual Voltage Vectors. The standard FSMPC uses $\lambda_{sc} > 0$ and thus it cannot use the fast optimization. This controller will be referred to as FSMPC-Basic. The VVV method uses a reduced cost function with lower computational load than FSMPC-Basic. The load reduction is achieved by removing the λ_{xy} factor as $x - y$ currents are treated in open loop. Also, the number of possible control moves is reduced from 32 (in FSMPC-Basic) to just 11, corresponding to the 10 active M + L VVV plus the inactive or zero VV. This controller will be referred to as FSMPC-VVV. Finally, the proposal uses a fast computation method considering all 32 basic VVs and the full CF. This controller will be referred to as FSMPC-Prop.

A summary of the experimental results can be found in Table 3. The performance indicators for each controller are presented. The characteristics of the operating points (A)

to (D) used in Table 3 are as follows: (A) is characterized by high values of both load and speed, (B) features a high load but at lower speed, (C) features medium values for both speed and load, and (D) uses low values of speed and load.

The entries of Table 3 show that the proposal produces lower values for tracking errors while maintaining the ASF below the VSI limit (10 kHz). It is worth observing that $E_{\alpha-\beta}$ values are notably reduced by the proposal. Operating points of high speed and load benefit the most from said reduction.

Table 3. Performance indicators for the basic FSMPC algorithm (left), for a multi-vector approach (middle) and for the proposal (right).

Op. Pt.	$E_{\alpha-\beta}$ **(mA)**	E_{x-y} **(mA)**	ASF **(kHz)**	$E_{\alpha-\beta}$ **(mA)**	E_{x-y} **(mA)**	ASF **(kHz)**	$E_{\alpha-\beta}$ **(mA)**	E_{x-y} **(mA)**	ASF **(kHz)**
(A)	241.07	134.12	2.77	312.01	59.94	7.52	157.00	91.20	5.97
(B)	82.52	109.91	6.03	114.11	59.82	9.94	62.42	75.34	8.85
(C)	94.29	121.31	5.74	102.12	59.87	9.81	63.96	76.27	8.96
(D)	80.33	117.35	6.06	97.78	59.95	10.0	59.37	87.38	8.90
Avg.	124.55	120.67	5.15	156.51	59.89	9.32	83.94	89.81	8.14
	FSMPC-Basic			FSMPC-VVV			FSMPC-Prop		

In addition, Figure 4 shows the experimental waveforms for the proposed method in $\alpha-\beta$ and $x-y$ planes. It can be seen that the sinusoidal trajectory of $\alpha-\beta$ stator currents is followed as expected. Also, the $x-y$ content is regulated during operation in closed loop.

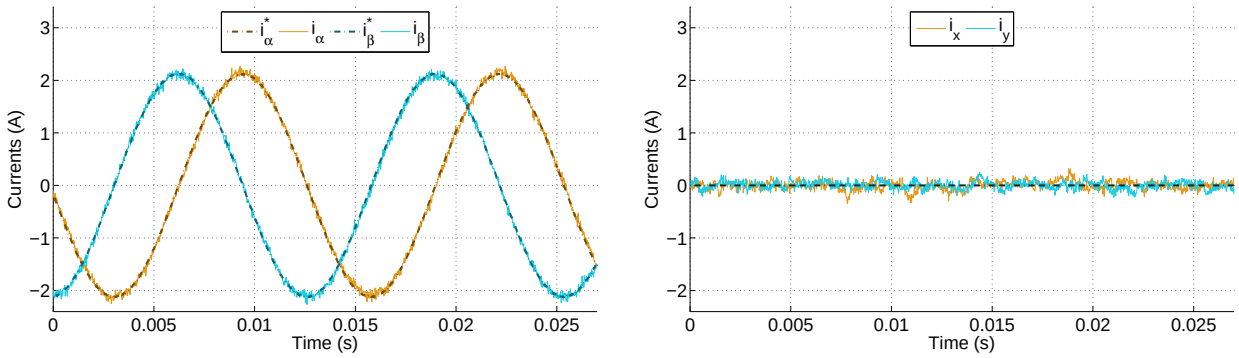


Figure 4. Waveforms obtained for the proposed controller in $\alpha-\beta$ (**left**) and $x-y$ (**right**) coordinates.

It is interesting to compare the waveforms obtained by the proposal and by a standard FSMPC. Figure 5 shows the waveforms for (a) standard FSMPC and (b) the proposed method. It can be seen that the FSMPC-basic method does not produce as good tracking as the proposal due to the fact that the optimization process limits the sampling frequency, having a negative effect. Also in Figure 5, the FSMPC-VVV has a slightly better performance than FSMPC-basic but it also has the problem of a reduced set of control actions. As a result, the best tracking is obtained by the proposal.

It is also interesting to check the flexibility of the proposal to trade switching frequency with tracking accuracy. This is enabled by the weighting factors in the cost function. In order to show this capability Table 4 shows the increase in current ripple when the switching frequency is diminished. Please note that for the proposal, a wide range of switching frequencies are available thanks to the fast method used in the optimization of the cost function.

The reduction in computational time provided by the proposed algorithm is shown in Table 5. The processor times for different tasks are shown divided among the various tasks that must be completed in real time every sampling period. The difference between FSMPC-Basic and FSMPC-Prop is highlighted. As expected, this difference is only visible

in the optimization phase. The total processing time is reduced from 36.91 (µs) for FSMPC-Basic to just 17.72 (µs) for the proposal. This reduction allows for a better control of stator currents as shown in Table 3.

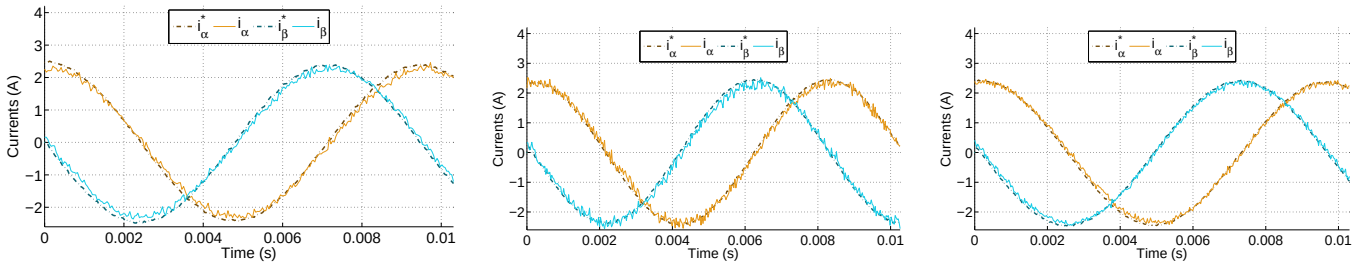


Figure 5. Comparison of waveforms for FSMPC-basic (**left**), FSMPC-VVV (**middle**) and FSMPC-Prop (**right**).

Table 4. Relationship between allowed ASF and current ripple $E_{\alpha-\beta}$.

ASF (kHz)	3.41	4.20	5.10	6.05	7.96	9.10
$E_{\alpha-\beta}$ (mA)	126.44	107.57	93.07	83.61	74.59	71.75

Table 5. Processor times for the algorithms.

Task	**FSMPC-Basic (µs)**	**FSMPC-Prop (µs)**
A/D conversion	2.14	2.14
PI + delay compensation	1.80	1.80
Optimization	25.80	**6.61**
Data logging	7.15	7.15
Total	36.91	**17.72**

Bold values indicate execution time improvement over the basic FSMPC.

The above results show that the proposal achieves fast computation. This can be translated to reduced sampling periods, with improved control results. Now, because the frequency term in the cost function is not neglected, the resulting switching frequency can be maintained at a reduced level. In this way the associated commutation losses are kept low and the hardware limitations are not violated.

In addition to the steady-state tests, a step test is performed to check the performance of the proposal. Please note that transient results are dominated by the PI in the outer loop. In the comparison this PI is the same for all controllers, otherwise some bias will be introduced. From these two factors, similar results are expected regarding transient tests. Figure 6 shows the mechanical speed and torque producing current evolution during a step change in speed reference. As can be seen, the proposal is slightly better than the basic FSMPC. The reason is the better current production by the proposal.

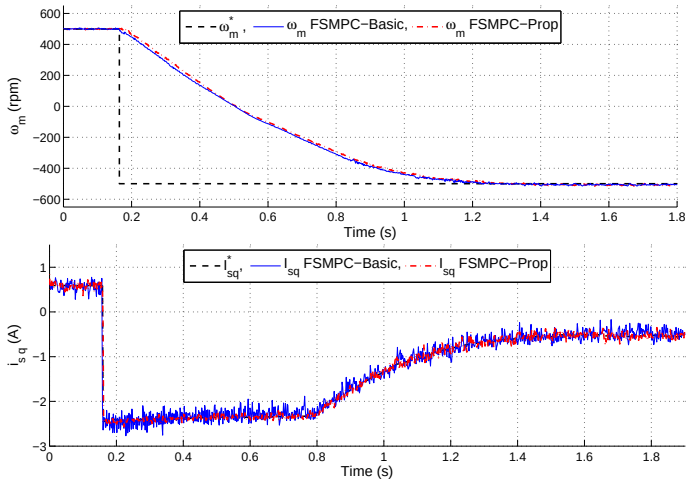


Figure 6. Speed step test results for the proposal and the standard FSMPC methods.

5. Conclusions

The field of model-based control is evolving from the basic algorithm and shifting toward more advanced methods that tackle specific problems of electric drives. Specifically, switching frequency in converter-supplied systems has become a focal point of recent research. Although model-based methods offer the flexibility to include switching frequency as an objective, real-time implementation is hindered by the high computational load. Previous methods sacrifice the switching frequency term to maintain real-time feasibility; however, this constitutes an important problem due to associated switching losses and thermal stress in the converter. This work introduces a solution that bridges this gap by retaining the switching objective without compromising computational efficiency.

The proposed method aims at retaining the low computational load while considering the switching frequency objective. In addition the method can benefit from recent proposals for weighting factor selection unlike other approaches. The experimental results state the viability of the proposal. In particular it has been shown that the fast minimization of the cost function is possible with the proposed method. The benefits seen in the experimental results stem from the reduced sampling period. Said reduction is achieved by the use of the region-based algorithm and cannot be achieved by the exhaustive exploration methods.

The experimental results also point in the direction of previous findings by the authors about the trade-off between figures of merit in FSMPC. These findings were made using exhaustive exploration. This hints at future work to fully corroborate these trade-offs for fast optimization algorithms.

Author Contributions: Conceptualization, M.R.A.; methodology, M.G.S., F.C. and A.P.V.-L.; software, M.G.S. and A.P.V.-L.; validation, M.R.A. and F.C.; formal analysis, M.R.A.; investigation, M.G.S., M.R.A. and F.C.; resources, M.R.A.; data curation, M.G.S.; writing—original draft preparation, M.G.S., M.R.A. and F.C.; writing—review and editing, M.G.S., M.R.A. and A.P.V.-L.; visualization, M.G.S. and A.P.V.-L.; supervision, M.R.A.; project administration, M.R.A.; funding acquisition, M.R.A. All authors have read and agreed to the published version of the manuscript.

Funding: This research received no external funding.

Informed Consent Statement: Not applicable.

Data Availability Statement: The original contributions presented in this study are included in the article. Further inquiries can be directed to the corresponding author.

Conflicts of Interest: The authors declare no conflicts of interest.

Abbreviations

The following abbreviations are used in this manuscript:

BVV	Basic Voltage Vector
CF	Cost Function
DC	Direct Current
FFSMPC	Fast Finite State Model Predictive Control
FSMPC	Finite State Model Predictive Control
IM	Induction Machine
MPC	Model Predictive Control
RMS	Root Mean Squared
VSI	Voltage Source Inverter
WF	Weighting Factor

References

1. Borreggine, S.; Monopoli, V.G.; Rizzello, G.; Naso, D.; Cupertino, F.; Consoletti, R. A review on model predictive control and its applications in power electronics. In Proceedings of the 2019 AEIT International Conference of Electrical and Electronic Technologies for Automotive (AEIT AUTOMOTIVE), Turin, Italy, 2–4 July 2019; pp. 1–6.
2. Elmorshedy, M.F.; Xu, W.; El-Sousy, F.F.M.; Islam, M.R.; Ahmed, A.A. Recent Achievements in Model Predictive Control Techniques for Industrial Motor: A Comprehensive State-of-the-Art. *IEEE Access* **2021**, *9*, 58170–58191. [CrossRef]
3. Mossa, M.A.; Mahmoud, H.; Hassan, A.A.; AL-Sumaiti, A.S. Dual-Mode Optimal Predictive Control of a Wind Driven Multi-Phase PMSG: A Hybrid Approach to Grid and Standalone Applications. *Results Eng.* **2025**, *28*, 107105. [CrossRef]
4. Lim, C.-S.; Levi, E.; Jones, M.; Rahim, N.A.; Hew, W.-P. A Comparative Study of Synchronous Current Control Schemes Based on FCS-MPC and PI-PWM for a Two-Motor Three-Phase Drive. *IEEE Trans. Ind. Electron.* **2014**, *61*, 3867–3878. [CrossRef]
5. Ouanouki, A.; Kouzi, K.; Difi, D.; Ghibeche, M. Predictive Control Strategy for Two Five-Phase Permanent Magnet Synchronous Motors Connected in Series Powered by A Single Inverter. *Int. J. Robot. Control Syst.* **2025**, *5*, 2311–2324. [CrossRef]
6. Colodro, F.; Torralba, A. Linearity enhancement of VCO-based quantizers for SD modulators by means of a tracking loop. *IEEE Trans. Circuits Syst. II Express Br.* **2014**, *61*, 383–387. [CrossRef]
7. Guo, Y.; Jiang, F.; Wang, S.; Cheng, S.; Hu, Z. Variable Control Period Model Predictive Current Control with Current Hysteresis for Permanent Magnet Synchronous Motor Drives. *Actuators* **2025**, *14*, 517. [CrossRef]
8. Liu, X.; Qiu, L.; Wu, W.; Ma, J.; Fang, Y.; Peng, Z.; Wang, D. Neural predictor-based low switching frequency FCS-MPC for MMC with online weighting factors tuning. *IEEE Trans. Power Electron.* **2021**, *37*, 4065–4079. [CrossRef]
9. Ait Ali, Y.; Ouassaid, M. Optimal FCS-MPC Cost Function Dimension Unification for Optimizing Operating Conditions of DFIG-Based Wind Turbine Power Converters. *IEEE Trans. Ind. Appl.* **2025**, 1–15. [CrossRef]
10. Arahal, M.R.; Satué, M.G.; Barrero, F.; Martinez-Heredia, J. Model Reference Adaptive Predictive Current Control of Six-Phase Induction Machine. *IEEE Trans. Ind. Electron.* **2025**, *72*, 10927–10934. [CrossRef]
11. Rodas, J.; Gonzalez, O.; Maidana, P.; Medina, C.; Doval-Gandoy, J.; Norambuena, M.; Ayala, M.; Rodriguez, J. Sequential model predictive torque control for six-phase machines without weighting factors. *IEEE Open J. Power Electron.* **2025**, *6*, 802–810. [CrossRef]
12. Gong, C.; Hu, Y.; Ma, M.; Gao, J.; Shen, K. Novel analytical weighting factor tuning strategy based on state normalization and variable sensitivity balance for PMSM FCS-MPTC. *IEEE ASME Trans. Mechatronics* **2020**, *25*, 1690–1694. [CrossRef]
13. Wang, S.; Zhang, Y.; Wu, D.; Zhao, J.; Hu, Y. Model predictive current control with lower switching frequency for permanent magnet synchronous motor drives. *IET Electr. Power Appl.* **2022**, *16*, 267–276. [CrossRef]
14. Xia, C.; Zhou, Z.; Wang, Z.; Yan, Y.; Shi, T. Computationally efficient multi-step direct predictive torque control for surface-mounted permanent magnet synchronous motor. *IET Electr. Power Appl.* **2017**, *11*, 805–814. [CrossRef]
15. Mamdouh, M.; Abido, M.A. Simple predictive current control of asymmetrical six-phase induction motor with improved performance. *IEEE Trans. Ind. Electron.* **2022**, *70*, 7580–7590. [CrossRef]
16. Abbaszadeh, A.; Arab Khaburi, D.; Kennel, R.; Rodríguez, J. Hybrid exploration state for the simplified finite control set-model predictive control with a deadbeat solution for reducing the current ripple in permanent magnet synchronous motor. *IET Electr. Power Appl.* **2017**, *11*, 823–835. [CrossRef]
17. He, Y.; Tang, Y.; Chen, Q.; Wang, F.; Kennel, R. Deadbeat Direct Power Control of Voltage-Sourced Rectifier with Reduced Switching Frequency. In Proceedings of the 2020 23rd International Conference on Electrical Machines and Systems (ICEMS), Hamamatsu, Japan, 24–27 November 2020; pp. 1511–1515.

18. Xu, Z.; Wang, Z.; Wang, X.; Cheng, M. Predictive current control method for dual three-phase PMSM drives with reduced switching frequency and low-computation burden. *IET Electr. Power Appl.* **2020**, *14*, 668–677. [CrossRef]
19. Rohten, J.A.; Dewar, D.N.; Zanchetta, P.; Formentini, A.; Munoz, J.A.; Baier, C.R.; Silva, J.J. Multivariable deadbeat control of power electronics converters with fast dynamic response and fixed switching frequency. *Energies* **2021**, *14*, 313. [CrossRef]
20. Dai, S.; Wang, J.; Sun, Z.; Chong, E. Deadbeat predictive current control for high-speed permanent magnet synchronous machine drives with low switching-to-fundamental frequency ratios. *IEEE Trans. Ind. Electron.* **2021**, *69*, 4510–4521. [CrossRef]
21. Gonzalez, O.; Doval-Gandoy, J.; Ayala, M.; Rodas, J.; Maidana, P.; Medina, C.; Romero, C.; Delorme, L.; Gregor, R.; Maciel, R. Virtual-vector-based predictive torque control for six-phase IM with reduced computational burden and copper losses. *IEEE Open J. Power Electron.* **2025**, *6*, 1371–1381. [CrossRef]
22. Zhou, H.; Xiang, X.; Li, Y.; Tao, T. Simplified model predictive current control for dual three-phase PMSM with low computation burden and switching frequency. *CES Trans. Electr. Mach. Syst.* **2024**, *8*, 447–454. [CrossRef]
23. Yuan, Q.; Xiao, R.; Wang, J.; Xia, K.; Yu, W. Double-virtual-vector-Based model predictive torque control for dual three-phase PMSM. *Electronics* **2024**, *14*, 50. [CrossRef]
24. Dong, Z.; Liu, C.; Song, Z.; Liu, S. Suppression of dual-harmonic components for five-phase series-winding PMSM. *IEEE Trans. Transp. Electrif.* **2021**, *8*, 121–134. [CrossRef]
25. Yu, B.; Song, W.; Yang, K.; Guo, Y.; Saeed, M.S. A computationally efficient finite control set model predictive control for multiphase PMSM drives. *IEEE Trans. Ind. Electron.* **2021**, *69*, 12066–12076. [CrossRef]
26. Cui, J.; Tao, T.; Zhao, W. Optimized Control Set Model Predictive Control for Dual Three Phase PMSM With Minimum Error Duty Cycle Regulation. *IEEE Trans. Power Electron.* **2023**, *39*, 1319–1332. [CrossRef]
27. Li, T.; Sun, X.; Lei, G.; Guo, Y.; Yang, Z.; Zhu, J. Finite-control-set model predictive control of permanent magnet synchronous motor drive systems—An overview. *IEEE CAA J. Autom. Sin.* **2022**. *9*, 2087–2105. [CrossRef]
28. Wang, B.; Jiao, J.; Xue, Z. Implementation of Continuous Control Set Model Predictive Control Method for PMSM on FPGA. *IEEE Access* **2023**, *11*, 12414–12425. [CrossRef]
29. Mousavi, M.S.; Davari, S.A.; Flores, F.; Garcia, C.; Rodriguez, J. ABC Frame Model-Free Predictive Control for Multiphase Converters and Electrical Drives. In Proceedings of the 2023 IEEE International Conference on Predictive Control of Electrical Drives and Power Electronics (PRECEDE), Wuhan, China, 16–19 June 2023; pp. 1–6.
30. Doi, M.V.; Nguyen, B.X.; Nguyen, N.V. A finite set model predictive current control for three-level NPC inverter with reducing switching state combination. In Proceedings of the 2019 IEEE 4th International Future Energy Electronics Conference (IFEEC), Singapore, 25–28 November 2019; pp. 1–9.
31. Arahal, M.R.; Barrero, F.; Satué, M.G.; Bermúdez, M. Fast Finite-State Predictive Current Control of Electric Drives. *IEEE Access* **2023**, *11*, 12821–12828. [CrossRef]
32. Xia, C.; Liu, T.; Shi, T.; Song, Z. A simplified finite-control-set model-predictive control for power converters. *IEEE Trans. Ind. Inform.* **2013**, *10*, 991–1002.
33. Andino, J.; Arcos-Aviles, D.; Guinjoan, F. Fast-execution neural-network-based modulated model predictive control for a three-phase three-level inverter. *Control Eng. Pract.* **2025**, *165*, 106595. [CrossRef]
34. Arahal, M.; Satué, M.; Barrero, F. Multi-phase weighted stator current tracking using a hyper-plane partition of the control set. *Control Eng. Pract.* **2024**, *153*, 106114. [CrossRef]
35. Cornell, E.P.; Lipo, T.A. Modeling and design of controlled current induction motor drive systems. *IEEE Trans. Ind. Appl.* **1977**, *IA-13*, 321–330. [CrossRef]

Disclaimer/Publisher's Note: The statements, opinions and data contained in all publications are solely those of the individual author(s) and contributor(s) and not of MDPI and/or the editor(s). MDPI and/or the editor(s) disclaim responsibility for any injury to people or property resulting from any ideas, methods, instructions or products referred to in the content.